Articles in PresS. Am J Physiol Regul Integr Comp Physiol (May 17, 2017). doi:10.1152/ajpregu.00351.2016

Flexible ammonia handling strategies using both cutaneous and branchial epithelia in the highly ammonia tolerant Pacific hagfish.

Alexander M. Clifford[1,2], Alyssa M. Weinrauch[1,2], Susan L. Edwards[2,3], Michael P. Wilkie[2,4], Greg G. Goss[1,2]

1. Department of Biological Sciences, University of Alberta, 116 St. and 85 Ave., Edmonton, Alberta, T6G 2R3, Canada
2. Bamfield Marine Sciences Centre, 100 Pachena Rd., Bamfield, British Columbia, V0R 1B0, Canada
3. Department of Biology, Appalachian State University, Boone, North Carolina, 28608-2027, USA
4. Department of Biology and Laurier Institute for Water Science, Wilfrid Laurier University, Waterloo, Ontario, N2L 3C5
* Author for correspondence (alex.clifford@ualberta.ca)

Running Title: Flexible ammonia handling by Pacific Hagfish

Key words: Cyclostome, Agnatha, Rhesus glycoprotein, Nitrogen, Skin

Copyright © 2017 by the American Physiological Society.

Abstract

Hagfish consume carrion, potentially exposing them to hypoxia, hypercarbia, and high environmental ammonia (HEA). We investigated branchial and cutaneous ammonia handling strategies by which Pacific hagfish (*Eptatretus stoutii*) tolerate and recover from high ammonia loading. Hagfish were exposed to HEA (20 mmol L^{-1}) for 48 h to elevate plasma total ammonia (T_{Amm}) levels before placement into divided chambers for a 4 h recovery period in ammonia-free seawater where ammonia excretion (J_{Amm}) was measured independently in the anterior and posterior compartments. Localized HEA exposures were also conducted by subjecting hagfish to HEA in either the anterior or posterior compartments. During recovery, HEA-exposed animals increased J_{Amm} in both compartments, with the posterior compartment comprising ~20% of the total J_{Amm} compared to ~11% in non-HEA exposed fish. Plasma T_{Amm} increased substantially when whole hagfish, and the posterior regions, were exposed to HEA. Alternatively, plasma T_{Amm} did not elevate following anteriorly-localized HEA exposure. J_{Amm} was concentration-dependent (0.05-5 mmol L^{-1}) across excised skin patches at up to 8-fold greater rates than in skin sections that were excised from HEA-exposed hagfish. Skin excised from more posterior regions displayed greater J_{Amm} than those from more anterior regions. Immunohistochemistry with hagfish-specific anti-rhesus glycoprotein type c (α-hRhcg; ammonia transporter) antibodies was characterized by staining on the basal aspect of hagfish epidermis while Western blotting demonstrated greater expression of Rhcg in more posterior skin sections. We conclude that cutaneous Rhcg proteins are involved in cutaneous ammonia excretion by Pacific hagfish, and that this mechanism could be particularly important during feeding.

Introduction

Hagfishes are distributed throughout the world's oceans, and along with the lampreys, are one of two families of extant jawless fishes that diverged from the vertebrate lineage approximately 500 million years ago (2). Hagfishes are also well-known scavengers, feeding on carrion that falls to the ocean bottom (35). Feeding opportunities may include marine mammals (44) and more commonly, fishes, including commercial by-catch (17). Adaptations for this feeding lifestyle include a protrusible dental plate capable of tearing flesh and burrowing into carrion (11), high tolerance to hypoxic and anoxic conditions (18), and the ability to acquire amino acids (26) and phosphate (42) across the skin and gill epithelia, in addition to the intestine (For review see 13). The high tolerance to ammonia observed in hagfishes may be related to their scavenging lifestyle, by which they may routinely encounter extremely high concentrations of ammonia while burrowing into the decomposing carcasses of fishes and large marine mammals (13, 14, 46). Currently there are no data characterizing the biochemical processes of putrefaction during marine-based decomposition. However, in terrestrial environments, mammalian decomposition produces high amounts of putrefactive compounds including hydrogen sulphide, methane, amino acids and pertinent to the current study, $(NH_4)_2SO_4$, which is deposited in the surrounding soil at levels exceeding 525 μg g^{-1} (~29 mmol L^{-1}; 7). As many of the microflora involved in the putrefactive process arise from the gut (7), it is reasonable to infer that decomposing aquatic organisms also produce high amounts of ammonia, and that immersion of the branchial region of hagfishes into the carcass would subject this region to high amounts of ammonia, which would result in the accumulation of ammonia in the hagfish. In

contrast, the posterior region of the animal is usually left exposed to seawater where the concentration of ammonia would be lower and likely favor excretion, provided that the appropriate transport mechanisms and gradients are present.

In most teleost fishes, ammonia toxicity arises when plasma ammonia concentrations exceed 1 mmol L^{-1}, leading to gill damage, metabolic disturbances, and disruption of the central nervous system as characterized by pronounced swelling of the brain (54), hyper-excitability, coma, and eventually death (see 29, 43, 50 for reviews). A number of tropical fishes however, including the weatherloach (*Misgurnus anguilla caudatus;* 9, 48), mudskipper (*Periophthalmodon schlosseri*; 30), and snakehead (*Channa asiatica*; 10) can withstand exposure to ammonia concentrations ranging up to 100 mmol L^{-1}. The ammonia tolerant Pacific hagfish (*Eptatretus stoutii*) readily survives 48 h exposure to 20 mmol L^{-1} total ammonia (T_{Amm}), which results in plasma ammonia concentrations of 5.7 mmol L^{-1}, the highest amount reported in any chordate (14). Furthermore, hagfish are also apparently capable of excreting ammonia against large, inwardly directed gradients during HEA exposure through active excretion (14). While the mechanism(s) responsible for this capability remains elusive, the potential exists that the gills and/or skin of the hagfish can be relatively impermeable to ammonia which may aid in their ammonia handling abilities.

The overarching goal of the present study was to investigate the relative roles of the gill and skin of Pacific hagfish in ammonia uptake and excretion during and following exposure to HEA. We hypothesized that there are differential nitrogen handling strategies employed between the anterior and posterior segments of the Pacific hagfish as a result of

88 their immersing themselves into carrion as they feed, which may incidentally lead to
89 ammonia uptake in the anterior (branchial) region, but excretion via posterior routes.

90 In the teleost gill, Rhcg (Rhesus glycoprotein type c) acts as a facilitated ammonia
91 transporter (SLC 42 transporter family; 56) and has been recently localized to the gill and
92 skin of Atlantic hagfish (*Myxine glutinosa*) and termed hRhcg (22). Similarly, the Pacific
93 hagfish gill has previously been shown to express Rhbg and Rhcg1 using
94 immunohistochemistry (IHC; 4). The presence of Rhcg in both the gill and skin of
95 hagfishes suggests that it likely plays an important role in modulating J_{Amm} by both
96 routes.

97 In the present study, the sites of ammonia flux (J_{Amm}) before, during and
98 following exposure to HEA (20 mmol L^{-1}) were measured in Pacific hagfish using
99 divided chambers to establish the relative role of anterior (branchial) vs. posterior (skin)
100 routes of ammonia uptake and excretion. Isolated skin patches were also used to measure
101 ammonia flux and Western blot and IHC were employed to investigate the mechanisms
102 of ammonia transport in the anterior and posterior regions of the hagfish. We were
103 particularly interested in determining whether Rhcg was differentially expressed along
104 the length of the skin of Pacific hagfish thereby providing a mechanistic understanding of
105 how J_{Amm} is facilitated in these ancient, highly ammonia-tolerant fishes.

106 **Materials and methods**

107 *Experimental animals and holding*

108 Pacific hagfish (*E. stoutii;* N = 78; average mass = 139.03 g; range = 95.85 –
109 199.45 g) were captured from Trevor channel near Bamfield, BC, Canada and held at

Bamfield Marine Sciences Centre (BMSC) as previously described (15). Hagfish were fasted for one week prior to experimentation to minimize the effects of postprandial nitrogenous waste production and excretion, and defecation on experiments. All animals were used under licenses of the Department of Fisheries and Oceans Canada (permit # XR-223 2013; XR-192 2014) and approved animal care protocol from BMSC (RS-13-24) and University of Alberta (00001126).

Chemicals

All chemicals, reagents and enzymes were purchased from Sigma-Aldrich Chemical Company (St. Louis, MO), unless otherwise noted.

Experimental protocols

Series 1: Sites of ammonia excretion following exposure HEA

Hagfish were transferred to 10.0 L, darkened buckets receiving continuously flowing seawater and left overnight to acclimate to the experimental set-up. The following morning, hagfish were removed, anesthetized (0.5 g L^{-1} tricaine methanesulfonate [TMS; Syndel Laboratories Ltd., Nanaimo, British Columbia, Canada] neutralized with 0.15 g L^{-1} NaOH) and a pre-exposure blood sample (200 µL) was drawn from the subcutaneous sinus using a heparinized 21G needle for blood and plasma acid/base/ammonia analysis. Immediately following blood sampling of lightly anesthetized hagfish, the animals were exposed to HEA (nominal [NH_4Cl] = 20 mmol L^{-1}; pH 7.5) in 5.0 L aerated seawater for 48 h. Simultaneous control (no HEA) animals were sampled and held in the same manner. After 48 h, both the control and HEA-

131 exposed hagfish were anesthetized, weighed and blood was collected as described above
132 with the puncture wound sealed using cyanoacrylate glue and a small square (~4 mm^2) of
133 nitrile rubber. Immediately following blood sample collection while hagfish were still
134 lightly anesthetized, animals were fitted into separating collar assemblies, briefly rinsed
135 in anesthesia-free seawater (~30 sec) to clear anesthetic, then placed into divided
136 chambers that isolated the posterior body region from the anterior region containing the
137 gill pores (see 15 for apparatus and protocol details). Nominally ammonia-free seawater
138 containing no anesthetic was then added to the anterior compartment only, and seal
139 efficacy checked by monitoring water appearance in the posterior compartment.
140 Ammonia-free seawater was then added to the posterior compartment and a lid secured.
141 The chamber was placed in a wet table receiving flowing seawater for temperature
142 control (~10 ˚C). Water samples (1 mL) for ammonia quantification were collected and
143 acidified to ~ pH 4.1 with 1 μL of 1 N HCl to prevent NH_3 volatilization and immediately
144 frozen following both the placement of hagfish into the chamber and following the 4 h
145 recovery period. After final sample collection, the patency of the seal was visually
146 inspected, the hagfish removed from the apparatus, killed by TMS overdose (5 g L^{-1} TMS
147 neutralized with 1.5 g L^{-1} NaOH), and a final blood sample collected (as above).

148 To evaluate the potential contribution of the cloaca to ammonia excretion, the
149 cloaca was sealed in a subset of experimental animals (n = 8) with a rubber bandage and
150 cyanoacrylate glue. No differences were detected in ammonia efflux in the posterior
151 compartment in animals with or without this seal.

152 To rule out artifacts, the divided chamber apparatus was leak-tested by measuring
153 Mg^{2+} flux as a proxy for leakage. Hagfish (n = 6) were fitted into the chambers (as

154 above), and artificial seawater (ASW; in mmol L^{-1} NaCl, 415; KCl, 10.2; Na_2SO_4, 28;
155 $CaCl_2$, 10; [pH = 8.0]) containing 50 mmol L^{-1} $MgCl_2$ was added to the anterior
156 compartment, and ASW containing 75 mmol L^{-1} $C_5H_{14}ClNO$ (choline chloride) to the
157 posterior compartment for osmotic balancing. An additional group of hagfish were also
158 placed into undivided chambers filled with Mg^{2+}-free seawater containing 75 mmol L^{-1}
159 $C_5H_{14}ClNO$ to determine endogenously derived branchial, cutaneous and cloacal Mg^{2+}
160 flux into the Mg^{2+}-free solution. All solutions were osmotically balanced with mannitol
161 (±1.0 mOsm kg^{-1}; VAPRO® vapor pressure osmometer, model 5520; Wescor Inc, Logan,
162 Utah, USA). No detectable movement of Mg^{2+} from the anterior-to-posterior chamber
163 over 4 h was observed, which ruled out any leakage between compartments (Mg^{2+}
164 detection limit of 0.94 μmol L^{-1}).

165

166 *Series 2: Localization of the routes of ammonia excretion following HEA.*

167 The effects of localized HEA exposure in anterior vs. posterior body regions were
168 determined by exposing each region individually to HEA and measuring ammonia flux in
169 the other compartment. Hagfish were sampled for blood and placed in the divided
170 chambers, followed by addition of sufficient NH_4Cl stock solution (1 mol L^{-1} prepared in
171 autoclaved seawater) to either the anterior or posterior compartment to yield a [T_{Amm}] of
172 20 mmol L^{-1}. Water samples were drawn immediately in the opposing compartment, and
173 again after 4 h, acidified and stored at -20˚C until further analysis. The animals were then
174 removed and blood samples collected for pH and T_{Amm} measurement.

175 *Series 3: The skin as a route of ammonia excretion.*

176 Measurements of J_{Amm} were made on patches of skin using the method described
177 by Glover et al. (26). Hagfish were held in ammonia-free seawater or exposed to HEA
178 (20 mmol L^{-1} NH_4Cl) for 48 h, then killed by TMS overdose (as above). The skin, dorsal
179 to slime glands running the length of the body from the ~5th branchiopore to the tail, was
180 removed, and 5 skin patches bisected by the dorsal midline (~3 cm X ~3 cm) were
181 prepared. Samples of skin were also fixed for immunohistochemistry (see below). Skin
182 patches were maintained in aerated saline (in mmol L^{-1}: NaCl, 474; KCl, 8; $MgCl_2$, 9;
183 $MgSO_4$, 3; NaH_2PO_4, 2.06; $NaHCO_3$, 5; HEPES, 20; glucose, 5; [pH = 7.8]) and used
184 within 1 h of excision. Each individual patch was placed over the top of the flux vial, and
185 secured in place with the serosal (basal) side of the skin facing outward. The inverted
186 chamber was then placed in a small plastic bottle (serosal bath) containing 20 mL of
187 hagfish saline containing different [T_{Amm}] (0.05, 0.1, 0.5, 1.0, 5.0 mmol L^{-1}). The inner
188 chamber of the vial served as the mucosal bath and was comprised of filtered, autoclaved
189 seawater. Serosal and mucosal solutions were independently mixed using a pipette and
190 continual aeration was provided throughout the flux period whereby the direction of flux
191 was from the serosal bath to the mucosal bath. Mucosal water samples (1 mL) were
192 drawn at the beginning and end of each flux measurement period (0, 2 h). Water samples
193 were then acidified as above and stored at -20º C until further analysis.

194 In a second set of experiments, the ammonia excretion capacity of the skin was
195 determined along the length of the hagfish. Six patches of skin (~3 cm X ~3 cm) were
196 excised as above at regular intervals (~12% of total body length) along the longitudinal

axis of the body encompassing both anterior and posterior regions of the animal, and tested for differences in J_{Amm}.

Series 4: Role of Rh glycoproteins in ammonia excretion by Pacific hagfish.

Multi-species alignments for Rh glycoprotein were constructed (15 Rhbg and 13 Rhcg homologues; Table 1) using MUSCLE (ebi.ac.uk/Tools/msa/muscle/) and an HMM (Hidden Markov Model) profile for each isoform was determined using HMMER3 (v3.0; Janelia Farm; hmmer.janelia.org). With these profiles, HMMER searches were conducted through a translated hagfish gill/slime gland Illumina transcriptome (12) and results were BLAST analyzed on NCBI to verify Rh family homology. Searches resulted in a full-length sequence for Pacific hagfish Rhcg (*E. stoutii* Rhcg; including 5' and 3' untranslated regions [UTRs]) and two partial sequences for Rh-like (Rh-like; sequence 1 containing 5' UTR and sequence 2 containing 3'UTR). The previous designation of hRhcg (22) does not take into account the different genera and species of hagfish; thus, we propose to term these newly cloned/sequenced Rh transcripts as *Es*Rhcg and *Es*Rh-like and these isoform identities were confirmed *via* phylogenetic analysis (see results). Using this sequence information, PCR primers were constructed using the UTRs (Table 2) to confirm full-length coding sequence (CDS) *via* cloning (see below).

Series 5: Determination of cutaneous EsRhcg abundance along the length of the animal

Hagfish that were not previously exposed to experimental HEA were terminally anesthetized (as above). Animals were then weighed and total animal length was recorded. Skin was excised at three locations (anterior, middle and posterior) at measured lengths from the snout of the animal. Excised skin was immediately transferred to a 2 mL

eppendorf tube containing RNAlater. Samples were then stored at -20 ˚C until protein expression analysis could be determined by electrophoresis and Western blot.

Analytical methods

Blood sample analysis

Immediately following blood collection, blood pH was measured using a thermojacketed (10 ˚C) Orion ROSS Micro pH electrode (Fisher Scientific, Ottawa, ON). The blood samples were then centrifuged (12,000 *g* for 30 seconds), and the plasma stored at -80 ˚C for T_{Amm} analysis. Plasma T_{Amm} concentration was quantified enzymatically using a commercial kit (Sigma-Aldrich Procedure A001) at 340 nm.

Water chemistry

Water ammonia concentrations were determined colorimetrically using the salicylate-hypochlorite assay at 650 nm (49), with a microplate spectrophotometer (Spectramax 190, Molecular Devices, Sunnyvale, CA) as previously described (14). Samples for Mg^{2+} quantification (Series 2) were analyzed using an atomic absorption spectrophotometer (Thermo Scientific model iCE 3300).

Molecular determination of EsRhcg and EsRh-like transcripts.

Total RNA was obtained from control hagfish gill (~100 mg) using TRIzol extraction. DNase I (Ambion/Life Technologies, Carlsbad, CA, USA) treated RNA was used to synthesize cDNA using RevertAid H-minus M-MuLV reverse transcriptase (Fermentas/Thermo Scientific, Pittsburgh, PA, USA). PCR reactions targeting full-length

CDS (coding DNA sequence) were conducted using Phusion DNA polymerase (Thermo Scientific, Pittsburgh, PA, USA) with species-specific primers (Table 2) for 35 cycles. Amplicons were analyzed by gel electrophoresis, imaged using Alpha Imager 2200, and gel purified using QIAquick Gel Extraction Kit (Cat. #28704). Products were cloned into *E.coli* (dh5-α) using the CloneJet PCR cloning kit (Thermo scientific, Pittsburgh, PA, USA). Plasmid DNA was isolated and sequenced at the University of Alberta.

Phylogenetic sequence analysis of cloned EsRhcg and EsRh-like transcripts

An alignment of the sequenced hagfish Rh glycoprotein homologues against Rh homologues from other species was conducted using MUSCLE (21) in SeaView (25, 27) for MacOS. The resulting alignment was then refined using GBlocks (8) to subtract gaps and residues of low/noisy homology with parameters selected to allow for more relaxed stringency (47). Phylogenetic analysis was conducted on the Cyberinfrastructure for Phylogenetic Research (CIPRES) Science Gateway servers (37) using RAxML version 8.0.9 (45) utilizing the LG evolutionary model (33). Branch support was estimated by bootstrap with 300 replications (auto-cutoff set at 1000 bootstraps). For phylogenetic analysis, base frequencies were model-determined and the proportion of invariable sites was determined using the GTRGAMMA model. A total of 85 protein sequences from the Rh glycoprotein family were collected from different species (including hagfish *Es*Rhcg and *Es*Rh-like protein sequences) and used in the analysis.

Histology and immunohistochemical detection of EsRhcg in skin tissue

Skin from non-HEA exposed hagfish (Series 3 experiments) was placed in fixative (4% paraformaldehyde in 10 mmol L^{-1} phosphate-buffered saline, pH 7.4) for 24

h at 4°C, rinsed (3X) in PBS then paraffin processed. Paraffin processed tissue was sectioned at 7 μm on a Leitz microtome and mounted on positively charged slides (Fisher Scientific). Sections were blocked (5% normal goat serum, and 0.1% Tween-20 in PBS at pH 7.4), then incubated with primary antibody hagfish anti-hRhcg (α-hRhcg; (22), diluted in blocking solution: α-hRhcg (1/500) overnight at room temperature, in a humidified chamber. Unbound primary antibody was removed by washing in PBS. Sections were then incubated with Alexa Fluor® goat anti-rabbit 568 (Molecular probes, Grand Island, NY) secondary antibody diluted in block for 1 h at RT. After rinsing for 15 min in PBS, sections were cover-slipped using Prolong® gold anti-fade reagent (Invitrogen, Grand Island, NY) and visualized using a Zeiss LSM510 Confocal Microscope.

Negative staining controls for *Es*Rhcg were processed in the absence of primary antibody and using pre-absorbed antibody incubations. In pre-absorbed controls, α-hRhcg was diluted to 1.25 μg mL^{-1} in blocking solution containing 2.5 μg mL^{-1} of α-hRhcg antigen. The antibody and peptide mixture was incubated at RT for 30 min before addition to tissue sections. Routine haematoxylin and eosin (H&E) staining was used for structural reference, using methods described by Weinrauch et al. (52).

Electrophoresis and Western blot analysis

Skin samples from Series 5 (stored in RNAlater) were pulverized under liquid nitrogen then transferred (~100 mg) to a centrifuge tube containing 1:10 w/v of ice-cold homogenization buffer (250 mmol L^{-1} sucrose, 1 mmol L^{-1} EDTA, 30 mmol L^{-1} Tris, 100 mg/mL PMSF, and 5 mg mL^{-1} protease inhibitor cocktail). Samples were then homogenized on ice using a hand-held motorized mortar and pestle (Gerresheimer

283 Kimble Kontes LLC, Dusseldorf, Germany) for 45 seconds. Homogenates were then
284 centrifuged at 3000 × *g* for ten minutes at 4 ˚C and the supernatant drawn off. A
285 subsample of the supernatant was assayed for protein determination *via* the BCA
286 (bicinchoninic) technique (Thermo Scientific, Rockford, IL, USA).

287 Processed gill samples were diluted with 3X Laemmli buffer (31) and 25 µg of
288 total protein was loaded in Criterion-TGX 20% acrylamide gels (Bio-Rad, Hercules, CA)
289 and separated by SDS-PAGE (sodium dodecyl sulfate, polyacrylamide gel
290 electrophoresis). Protein was transferred to a nitrocellulose membrane (Millipore,
291 Billerica, MA). Protein transfer was confirmed by soaking membranes in Ponsceau S
292 staining solution (0.1% (w/v) Ponceau S in 1% (v/v) acetic acid). Membranes were
293 washed (2 min in distilled water followed by 3 x 1min in 0.5 M Tris-Buffered Saline
294 [TBS; pH=8.0] containing 0.2% Tween-20 [TBST]) and then blocked in 5% blotto (5%
295 skim milk powder in TBST) on a shaking carousel overnight at 4 ˚C.

296 Membranes were washed (3 x 15 min in TBS and then 3 x 15 min in TBST)
297 before overnight incubation in blocking buffer containing 1˚ antibody (1:5000 rabbit anti-
298 *h*Rchg) at room temperature. Membranes were then washed 3 times (15 min in TBST)
299 and incubated with 2˚ antibody (1:10,000 goat anti-rabbit HRP; Santa Cruz
300 Biotechnologies Inc., Dallas, TX, USA) and Precision Protein StrepTactin-HRP
301 conjugate (Bio-Rad) in TBST at room temperature for 1 h. Membranes were washed 3
302 times (15 min) in TBST followed by a final wash in TBS. Labeled protein bands were
303 detected *via* enhanced chemiluminescence (ECL; Pierce; SuperSignal West Pico
304 Chemiluminescent Substrate; Rockford, Il, USA). Visualization occurred using Bio-Rad
305 Chemidoc system with densitometry analysis completed using image analysis software

306 (Bio-Rad). Standardization for protein concentration was quantified on the basis of 25 µg
307 of total protein loaded into each well.

308 *Calculations and statistical analysis*

309 Calculations of J_{Amm} were based on the T_{Amm} accumulation in the water in either
310 the anterior and/or posterior compartments using the following equation:

311 $$J_{Amm} = \left([T_{Amm}]_{final} - [T_{Amm}]_{initial} \cdot V\right) \cdot \frac{1}{m} \cdot \frac{1}{\Delta t} \qquad (1)$$

312 where $[T_{\mathrm{Amm}}]$ is the initial or final concentration of ammonia in the water (µmol L^{-1}); V
313 is the volume of water (mL); m is the animal mass (g) and Δt the duration of the flux
314 period.

315 Rates of J_{Amm} across excised hagfish skin were determined by measuring
316 ammonia appearance in the mucosal bath of the miniature flux chambers using the
317 following equation:

318 $$J_{Amm}^{Skin} = \left([T_{Amm}]_{final} - [T_{Amm}]_{initial} \cdot V\right) \cdot \frac{1}{SA} \cdot \frac{1}{\Delta t} \qquad (2)$$

319 where SA is the measured mucosal surface area of hagfish skin exposed to seawater
320 (cm^2), and other notations are as stated above.

321 When hagfish were placed in the divided chambers, ~40% of the hagfish skin was
322 in the anterior compartment whilst ~60% was in the posterior compartment. With this
323 partitioning in mind, rough estimates of branchial and cutaneous J_{Amm} rates ($J_{\mathrm{Amm}}^{\mathrm{branc}}$ and

$J_{\mathrm{Amm}}^{\mathrm{cutan}}$) were calculated from experimentally determined average anterior and posterior rates ($J_{\mathrm{Amm}}^{\mathrm{ant}}$ and $J_{\mathrm{Amm}}^{\mathrm{post}}$) as follows.

$$J_{\mathrm{Amm}}^{\mathrm{cutan}} = J_{\mathrm{Amm}}^{\mathrm{post}} + \left(\left(\frac{J_{\mathrm{Amm}}^{\mathrm{post}}}{60\%}\right) \cdot 40\%\right) \quad (3)$$

$$J_{\mathrm{Amm}}^{\mathrm{branc}} = J_{\mathrm{Amm}}^{\mathrm{ant}} - \left(\left(\frac{J_{\mathrm{Amm}}^{\mathrm{post}}}{60\%}\right) \cdot 40\%\right) \quad (4)$$

All data are presented as the mean ± s.e.m.. Differences between groups with respect to plasma T_{Amm}, blood pH were tested using two-way analysis of variance followed by Holm-Sidak's multiple comparison *post-hoc* tests. Differences in J_{Amm} for the divided chamber studies during recovery from HEA exposure were tested using one-way analysis of variance followed by Holm-Sidak's multiple comparison *post-hoc* tests. Differences in plasma T_{Amm} in localized HEA exposure studies were tested using a Kruskal-Wallis non-parametric test followed by Dunn's multiple comparisons test while differences in blood pH in this series were tested with one-way analysis of variance followed by Holm-Sidak's multiple comparison *post-hoc* test. Differences in anterior and posterior J_{Amm} in localized HEA-exposure experiments were tested with Student's one-tailed unpaired t-test with Welch's correction. Measurements of J_{Amm} across excised skin (skin from HEA vs. non-HEA hagfish) were compared using multiple Student's two-tailed t-test with a Holm-Sidak correction for multiple comparisons. Differences in skin J_{Amm} along the hagfish length were tested for by linear regression analysis. Differences in *Es*Rhcg abundance along the length of the skin were tested using one-way ANOVA followed by Holm-Sidak's multiple comparison *post-hoc* test. The fiducial limit of statistical significance was $p < 0.05$. All statistical analyses were completed using GraphPad Prism 6.0 (GraphPad Software, San Diego, USA).

Results

Series 1: Sites of J_{Amm} following HEA exposure

Plasma T_{Amm} was below the limit of detection in Pacific hagfish prior to HEA exposure, and did not rise significantly in the parallel control animals not exposed to HEA. Exposure to 20 mmol L^{-1} total ammonia (HEA) for 48 h resulted in no mortalities, but did lead to elevated plasma T_{Amm}, which increased to ~2600 μmol L^{-1} ($p < 0.0001$; Figure 1A) Following HEA exposure, subsets of animals were then allowed to recover for 4 h in ammonia-free sea water in divided chambers, with half of the animals fitted with a cloacal seal. By 4 h of recovery, plasma T_{Amm} was significantly reduced by approximately 30-40% regardless of the presence of the cloacal seal ($p < 0.0001$; Figure 1A).

In control (non-HEA exposed) hagfish, blood pH (Figure 1B) was unchanged following HEA ($p = 0.7816$) and was slightly elevated in the group of hagfish not fitted with the cloacal seal (Figure 1B; $p = 0.0016$), but not in those animals fitted with the seal (no HEA; $p = 0.3920$; Figure 1B). After 4 h recovery in ammonia free water, the hagfish with and without the cloacal seal experienced a slight metabolic acidosis characterized by respective reductions of 0.44 and 0.33 pH units, which were significantly lower than values measured immediately following HEA ($p < 0.0001$). It was notable that the control animals also underwent a slight metabolic acidosis following time-matched recovery in the divided chamber (~0.18 pH units; $p < 0.0001$).

When control hagfish, not exposed to ammonia, were placed in divided chambers, routine J_{Amm} averaged 40.0 ± 25.9 μmol kg^{-1} h^{-1} (Figure 2A) in the anterior compartment

and 4.9 ± 1.4 μmol kg^{-1} h^{-1} in the posterior compartment (Figure 2B). However, recovery from 48 h exposure to HEA resulted in rates of anterior J_{Amm} that were significantly greater (~15-fold) compared to controls, in both those hagfish that were not fitted with the cloacal seal (p = 0.0022) and those that were (p = 0.0022; Figure 2A). Excretion in the posterior compartment also increased significantly by ~30-fold in hagfish having no cloacal seal (p < 0.0001) and ~23 fold in those with the seal (p < 0.0001). No statistical differences in J_{Amm} were observed between animals with and without a cloacal seal in either the anterior (p = 0.7279) or posterior compartment (p = 0.1358). In HEA exposed animals, the posterior excretion represented ~19% of the total J_{Amm} (combined anterior plus posterior) in animals with no cloacal seal and ~17% in animals with a cloacal seal compared to approximately 11% in the non-exposed controls (Figure 2B).

Series 2: Localization of the routes of J_{Amm} following HEA.

Exposure of the anterior region of the hagfish to HEA for 4 h resulted in a plasma T_{Amm} load of ~80 μmol L^{-1} but was not significantly different (p = 0.5988) compared to concentrations measured in control (no HEA) animals, which were below detectable limits (Figure 3A). Notably, when the posterior end of the hagfish was exposed to HEA, animals experienced substantial (>1500 μmol L^{-1}) accumulations in plasma T_{Amm} compared to both control (p < 0.0001) and anteriorly HEA-exposed hagfish (~21-fold greater; p < 0.0074; Figure 3A).

While no differences in blood pH were observed following 4 h exposure of the anterior body to HEA compared to control animals (p = 0.7484), exposure of the

posterior body regions to HEA resulted in a significant acidosis compared to anteriorly HEA-exposed animals characterized by a 0.3 pH unit drop (p = 0.0443; Figure 3B).

When the route of HEA exposure was *via* either the anterior or posterior chamber, J_{Amm} was measured in the opposing HEA-free compartment. When HEA exposure was *via* the posterior compartment, anterior J_{Amm} was ~4-fold great than anterior rates in control animals (p = 0.0329; Figure 4A). When the route of HEA was *via* the anterior compartment, posterior J_{Amm} was ~25-fold greater than that measured in controls (p = 0.0085; Figure 4B).

Series 3: Ammonia flux across excised skin tissue

To further investigate the skin's role in ammonia handling, skin patches were excised from the dorsal region of hagfish exposed to HEA (20 mmol L^{-1}) for 48 h or from control animals held in ammonia-free seawater. In both cases J_{Amm} was measured while exposing the serosal side of the patches to a range of serosal T_{Amm} concentrations. Compared to the controls, J_{Amm} was significantly greater in skin patches excised from HEA-exposed hagfish at all but the highest T_{Amm} concentrations (10 mmol L^{-1}; p = 0.1786); notably, J_{Amm} across the skin excised from HEA-exposed animals was ~8-fold greater at a serosal [T_{Amm}] of 0.05 and 0.1 mmol L^{-1} (p = 0.0006 and p = 0.0135 respectively), ~4-fold greater at 0.5 and 1.0 mmol L^{-1} (p = 0.0027 and p = 0.0026 respectively) and 1.3-fold greater at a serosal [T_{Amm}] of 5 mmol L^{-1} (p = 0.0434; Figure 5A).

The skin contribution to J_{Amm} also appeared to be greater in posterior relative to anterior body regions, with J_{Amm} increasing linearly in skin sections sampled sequentially

411 from anterior to posterior (R^2= 0.88) with a slope of 0.1307 ± 0.024 ([nmol cm^{-1} h^{-1}]/[%
412 distance from snout]) that was significantly different from a slope of 0 ($F_{1,4}$ = 30.30,
413 p=0.00531) and an intercept of 18.82 ± 1.436 nmol cm^{-1} h^{-1} (Figure 5B).

414 *Series 4: Detection and distribution of EsRhcg in cutaneous tissue*

415 Using an Illumina transcriptome for combined gill/slime gland, a full-length
416 sequence for *Es*Rhcg and a partial *Es*Rh-like sequence was isolated. Using species-
417 specific primers generated from transcriptomic data, full-length amplicons were
418 amplified using PCR. Sequencing following subsequent cloning identified a 1386 bp
419 ORF (open reading frame) encoding a 462 amino acid residue protein for *Es*Rhcg
420 sequence and a 1443 bp ORF encoding a 481 amino acid protein for *Es*Rh-like sequence.
421 These sequences share high homology (>98% at amino acid level) with previously
422 identified homologues from Atlantic hagfish (22). Maximum-likelihood phylogenetic
423 analysis of these sequences against subfamilies of the Rh glycoprotein family
424 demonstrated that the cloned *Es*Rhcg and *Es*Rh-like are members of the Rh glycoprotein
425 family (Figure 6). Full-length sequences for cloned *Es*Rhcg and *Es*Rh-like sequences are
426 found on the NCBI database (accession numbers KT943755, KT943754 respectively).

427 H&E staining highlighted the cellular composition of the capillary (Cp)-rich
428 dermis (De) (20, 28, 32, 39, 53), as well as the prominent mucous cells (MC) in the basal
429 aspect of the epidermis (Ep; Figure 7A). Immunohistochemical analysis, using α-hRhcg
430 antibody (22), demonstrated that *Es*Rhcg immunoreactivity was more prominently
431 localized towards the basal aspect of the skin epidermis but not in the dermal layer
432 (Figure 7B). Peptide competition eliminated this staining in the epithelial layer but not

the non-specific staining in the dermal layer (Figure 7B inset). The Pacific hagfish *Es*Rhcg sequence exhibited 88% (15/17 amino acids) identity with the antigenic peptide sequence used to create α-hRhcg antibody (Table 3).

Series 5: Determination of relative cutaneous EsRhcg abundance along the length of the animal

Skin tissue excised sequentially from anterior to posterior was distributed on a percentage distance from snout basis (Anterior: 27.58 ± 0.9 %; Middle: 57.21 ± 1.40 %; Posterior: 84.19 ± 1.08 %). Western blot analysis on skin tissue using hagfish specific α-hRhcg antibody (22) yielded a single immunoreactive protein band at ~50 kDa (duplicate representative blot of each skin section shown in Figure 8A). Abundance of *Es*Rhcg was variable across the length of the skin and was statistically greater in skin sections excised from the middle of the trunk ($p = 0.0448$) and demonstrated an increasing trend in the posterior ($p = 0.0707$) sections of the animal compared to anterior sections (Figure 8B). No significant differences were observed between the middle and posterior sections ($p = 0.6677$).

Discussion

Hagfish have impressive capabilities to tolerate and excrete ammonia during HEA exposure (4, 14, 22, 23, 36). The present study demonstrates that following HEA exposure, hagfish excrete ammonia using both the gills and the skin. These findings are supported by the ~15-fold and ~23- to 30-fold greater rates of ammonia excretion that were observed in the anterior and posterior sections respectively, of the animals following

exposure to HEA for 48 h. Moreover, measurements of ammonia excretion on isolated skin patches demonstrated that the ammonia permeability of the skin increased along the length of the animal from anterior to posterior. Using immunocytochemistry, we also demonstrated that *Es*Rhcg is expressed in the epidermal layer of the skin of Pacific hagfish. This finding, taken together with our observation that *Es*Rhcg proteins were located immediately adjacent to the dermal capillaries, provides mechanistic evidence for ammonia transport via the skin. Differences in anterior and posterior J_{Amm} in localized ammonia exposure experiments matched the measured increases in J_{Amm} noted in more posterior skin sections in isolated skin flux studies. Importantly, these results also coincided with greater *Es*Rhcg expression in the middle and a trend (p = 0.0707) toward increased expression in posterior excised skin segments compared to anterior segments. We conclude that hagfish not only have the ability to differentially handle ammonia using both the gills and the skin, but also that the relative capacity of each route to excrete ammonia can be altered during, and following exposure to HEA.

Ammonia excretion across the gills and the skin likely involves Rhesus glycoproteins, as described in other fish species (56). This interpretation is supported by the identification of two Pacific hagfish Rh orthologs of the SLC42 family of transporters. Comprehensive phylogenetic analysis demonstrates that two orthologs are confidently rooted within the well-conserved Rh transport family. These two *Eptatretid* Rhs (*Es*Rhcg and *Es*Rh-like) plus the two previously identified *Myxinid* Rhs (hRhcg and hRhbg respectively) represent the earliest Rh proteins characterized in the extant vertebrate lineage. *Es*Rhcg clearly grouped with other Rhcg family members at the basal node for all other Rhcg homologues. A second sequence, defined as *Es*Rh-like, could not

478 be attributed to either the Rhag or Rhbg family, but it did group with low confidence with
479 Rh30-like proteins found in other teleost genomes.

480 Atlantic hagfish (*Myxine glutinosa*) express hRhcg not only in the gills, a
481 common site for ammonia excretion, but also in skin (22). The presence of an extensive
482 dermal capillary network (20, 28, 32, 39, 53) in hagfish skin is purported to be an
483 important site of gas exchange (39); although, this hypothesis has been challenged based
484 on the thickness of the skin (34) and a recent study clearly showing that Pacific hagfish
485 lack the ability to cutaneously take-up sufficient O_2 to satisfy routine metabolic demands
486 (16). In the current study, *Es*Rhcg was localized in the epidermal tissue in close
487 proximity (≤20 μM; Figure 7A,B) to the dermal capillaries in Pacific hagfish. Because
488 NH_3 is a much smaller molecule and approximately 10,000 times more soluble in water
489 than oxygen (3, 5), we hypothesize that *Es*Rhcg in hagfish, and its proximity to the
490 dermal capillaries provide a mechanism for facilitated transport of ammonia across the
491 skin that is not available for the transport of oxygen. The increasing permeability to
492 ammonia along the length of the skin from the anterior to posterior regions of the hagfish
493 (Figure 5B) also supports this hypothesis.

494 Based on our observations, we propose that during feeding, the more posterior
495 regions of hagfish skin have more favorable NH_3 diffusion gradients compared to the
496 anterior regions, which may be buried in the carrion upon which the hagfish are feeding.
497 During feeding events, there could be much higher concentrations of ammonia in the
498 adjacent water near the anterior (head plus gills) regions due to decomposition of the
499 carrion tissue and the more confined space, than in the more posterior regions, which are
500 more distal to the carrion. The posterior regions also appear to be more ammonia

permeable than the anterior regions, which may limit ammonia uptake via the gills/head region while simultaneously promoting offloading via the posterior regions whilst immersing themselves in their meals. Indeed, localized ammonia exposures demonstrate anterior (i.e. branchial) HEA exposure results in substantially less accumulation of plasma T_{Amm} (Figure 3A) than does equivalent posterior HEA exposure. In contrast, the rise in plasma ammonia, when the route of exposure is *via* the posterior chamber, indicates that hagfish are less able to limit posterior cutaneous ammonia uptake, at least acutely. While the mechanisms behind the differences in the permeability of the anterior vs. posterior regions of the hagfish remain unresolved, changes in gill ammonia permeability due to changes in *Es*Rhcg abundance can be ruled out. Western blots of gill tissue demonstrated that prolonged exposure of hagfish to identical ammonia concentrations used in the current study were not accompanied by changes of branchial *Es*Rhcg protein abundance (14).

Our results also demonstrate that regional differences in the cutaneous permeability to NH_3 may promote ammonia excretion in the posterior (cutaneous) regions of the hagfish when the anterior portions of its body are immersed in carrion during feeding (Figure 4B). Presumably, the posterior portion of the animal would face a lower environmental ammonia compared to the anterior portion in a feeding hagfish, which would facilitate a "flow-through" of ammonia from the anterior to the posterior of the animal. Unfortunately, reliable protein extracts could not to be obtained from frozen skin tissue from HEA and control fish. However, there were differences in *Es*Rhcg expression along the length of the animal with lower expression in anterior tissue and greater

523 expression in skin excised from the middle and arguably, the posterior (see above)
524 sections of the animal.

525 As facilitated transporters, Rh glycoproteins promote ammonia transport in a bi-
526 directional manner along prevailing NH_3 partial pressure gradients (6, 51). Such bi-
527 directional transport would be compatible with our proposed flow-through model. Under
528 normal conditions, the anterior portions of the unrestrained (free-swimming) hagfish
529 would facilitate the bulk of ammonia excretion. When hagfish are immersed in carcasses
530 during feeding however, the posterior regions would take on added importance to unload
531 ammonia that was inadvertently taken-up from the carcass itself or the surrounding
532 environment. Other factors including the extent of vascularization and local blood flow
533 could also affect delivery and the relative permeability of the skin and gills to ammonia,
534 and should also be examined to determine how/if these processes are modulated.
535 Nevertheless, the presence of *Es*Rhcg and its differential expression supports a
536 substantive role for the skin and posterior regions of the animal.

537 *Regional differences in J_{Amm} following HEA exposure*

538 During recovery in sea water following ammonia exposure, both the gill and skin
539 contributed to J_{Amm} in the anterior compartment, while cutaneous and cloacal (intestinal
540 and renal combined) constituents contributed to J_{Amm} in the posterior compartment. Our
541 experiments revealed that a cloacal seal did not impact J_{Amm} in the posterior chamber in
542 either control (15) or HEA exposed animals (Figure 2A), demonstrating that cloacal
543 efflux does not play a prominent role in J_{Amm}. Given the low urine flow-rate of the
544 hagfish (227 µl kg^{-1} h^{-1}; 38), the urine would have to be concentrated to >800 mmol L^{-1} to
545 account for the measured J_{Amm}. This would be ~2 orders of magnitude greater than the

546 hagfish plasma T_{Amm} following HEA exposure. Given that hagfish are osmoconformers
547 (19), have rudimentary kidneys (52) and have a urine composition similar to plasma (1),
548 it is unlikely that hagfish concentrate ammonia within their urine as a means of excretion;
549 thus, posterior flux rates we measured are interpreted as being primarily cutaneous.

550 Currently, there are no estimates of branchial (gill pouch) surface area in hagfish
551 so we are unable to empirically attribute flux of ammonia to either the skin or the gill
552 surface area. Estimation of gill ammonia permeability is further complicated by the fact
553 that there is considerable interspecies variation in the number of gill pouch pairs in *E.*
554 *stoutii* (10-13 pairs; 52) and other hagfishes (40). Furthermore, it is unknown whether
555 individual gill pouches along the length of the branchial region similarly express *Es*Rhcg.
556 For these reasons, we only refer to anterior versus posterior flux contributions with the
557 anterior portion obviously comprising both cutaneous and branchial components while
558 the posterior only being comprised of cutaneous exchange. Clearly, estimates of gill
559 surface area and investigations of the branchial Rh profile in hagfishes are required to
560 accurately attribute ammonia permeability to specific branchial versus cutaneous
561 contributions. That said, adjusting for the presence of skin in the anterior chamber (see
562 methods), rough estimates of cutaneous contributions to ammonia excretion were ~18%
563 of total routine rates and increased to ~30% following exposure to HEA. Given the
564 dynamic *Es*Rhcg profile and the changing J_{Amm} profile along the length of hagfish skin
565 and the arguments listed above, these estimates should be cautiously interpreted.
566 Cutaneous ammonia excretion has been observed in several fish species including dab
567 (*Limanda limanda*; 41), rainbow trout (*Oncorhynchus mykiss*; 57) and the mangrove
568 killifish (*Kryptolebian marmoratus*; 24). In trout, cutaneous ammonia excretion

accounted for 4.5% of total J_{Amm} under routine conditions and mildly increased to 5.7% following HEA exposure (12 h; 2 mmol L^{-1}; 57) while in the dab, cutaneous ammonia excretion accounted for 47% under routine conditions; however, the effect of ammonia loading *via* HEA exposure in dab has yet to be determined (41).

Acid/base response during exposure, recovery and localized exposure.

Exposure to high environmental ammonia is known to result in a metabolic alkalosis (elevated pH) which is compensated for over the next 12 hours by a compensatory retention of metabolic H^+ (55). However, during recovery in ammonia-free seawater, ammonia (NH_3) leaves preferentially and the result is an internal metabolic H^+ load (lowered pH) due to dissociation of NH_4^+ into NH_3 and H^+. Clifford et al. (14) reported a similar response in whole hagfish during similar HEA exposure. However, a perplexing result in the current study is the ~0.2 pH unit acidosis that was only observed following acute (4 h) posterior exposure to HEA and not with anteriorly-applied HEA. Posterior entry of NH_4^+ could account for this result. However, the entry of ammonia as NH_4^+ seems unlikely given the relatively low cationic permeability of the hagfish body surface (23). Current understanding of Rh-facilitated ammonia transport based on mammalian Rh's expressed in *Xenopus laevis* oocytes suggests that Rhcg only transports neutral NH_3, and is then trapped as NH_4^+ by H^+ excreted via branchial V-ATPases and/or NHE proteins (56). However, Caner et al. (6) also suggests that other isoforms of Rh protein (Rhbg, RhAG) are capable of transporting both neutral NH_3 and ionized NH_4^+ (6). The transporting capabilities of these hagfish isoforms with respect to substrate selectivity remain to be elucidated and provide avenues for future research with studies similar to those conducted by Caner et al. (6). A second possible explanation for the perplexing 0.2

pH unit acidosis still present after 4 h of posteriorly applied HEA is that the signal for acid-base regulation is branchially located and not stimulated by either posterior HEA application or elevated plasma ammonia. Clearly, the possibility of differentially activating acid-base regulatory responses by differential HEA application is intriguing and bears further investigation.

Perspective and Significance

This study demonstrates that there is regional variation in ammonia transport in the hagfish, and that the posterior regions of the hagfish may take on added importance when the anterior regions are exposed to high concentrations of ammonia, as could possibly occur when they are feeding on carrion. The expression of *Es*Rhcg protein in the epidermal tissue provides a mechanism by which ammonia can be transported across the thick epidermal layer that characterizes the trunk/posterior regions of the body. Furthermore, HEA-induced plasma ammonia loading results in a higher cutaneous permeability in excised skin suggesting that Pacific hagfish are able to differentially regulate the ammonia permeability of the gills and the skin. These adaptations, may allow the hagfish to unload ammonia that is inadvertently taken-up by the gills while feeding on decaying carrion, while simultaneously facilitating off-loading ammonia to the water via the skin in the more posterior regions of their body. Further investigation is necessary to identify the underlying mechanism responsible for this remarkable ability to limit ammonia uptake.

Acknowledgements

We thank Dr. Eric Clellend (Research Coordinator at BMSC) for his unwavering diligence in supporting this research, Rachel Munger for assistance in sample collection, and Sam Guffey, Chris Wood and Alex Zimmer for advice.

Competing interests

The authors declare no competing interests.

Funding

A.M.C. was supported by an NSERC-PGSD (370386) and Alberta Innovates Technology Futures studentship grant, The Andrew Stewart Memorial prize, The Donald M. Ross scholarship and R. E. Peter Memorial Scholarship, The Western Canadian Universities Marine Sciences Society Graduate Student Award and the Dick & Leona BMSC residential Bursary. G.G.G (203736) and M.P.W (194686) are supported by Natural Sciences and Engineering Council of Canada (NSERC) Discovery Grants. S.L.E is supported by the National Science Foundation Grant: Integrative Organismal Systems (1121369)

References

1. **Alt JM**, **Stolte H**, **Eisenbach GM**, **Walvig F**. Renal electrolyte and fluid excretion in the Atlantic hagfish *Myxine glutinosa*. *J Exp Biol* 91: 323–330, 1981.

2. **Bardack D**. First fossil hagfish (Myxinoidea): a record from the Pennsylvanian of Illinois. *Science* 254: 701–703, 1991.

3. **Boutilier RG**, **Heming TA**, **Iwama GK**. Appendix: Physicochemical parameters for use in fish respiratory physiology. In: *Gills - Anatomy, Gas Transfer, and Acid-Base Regulation*, edited by Hoar WS, Randall D. Orlando: Elsevier, 1984, p. 403–430.

4. **Braun MH**, **Perry SF**. Ammonia and urea excretion in the Pacific hagfish *Eptatretus stoutii*: Evidence for the involvement of Rh and UT proteins. *Comp Biochem Physiol A* 157: 405–415, 2010.

5. **Cameron JN**, **Heisler N**. Studies of ammonia in the Rainbow trout: Physico-chemical parameters, acid-base behaviour and respiratory clearance. *J Exp Biol* 105: 107–125, 1983.

6. **Caner T**, **Abdulnour-Nakhoul S**, **Brown K**, **Islam MT**, **Hamm LL**, **Nakhoul NL**. Mechanisms of ammonia and ammonium transport by rhesus-associated glycoproteins. *Am J Physiol Cell Physiol* 309: C747–58, 2015.

7. **Carter DO**, **Yellowlees D**, **Tibbett M**. Cadaver decomposition in terrestrial ecosystems. *Naturwissenschaften* 94: 12–24, 2007.

8. **Castresana J**. Selection of conserved blocks from multiple alignments for their use in phylogenetic analysis. *Mol Biol Evol* 17: 540–552, 2000.

9. **Chew SF**, **Jin Y**, **Ip YK**. The loach *Misgurnus anguillicaudatus* reduces amino acid catabolism and accumulates alanine and glutamine during aerial exposure. *Physiol Biochem Zool* 74: 226–237, 2001.

10. **Chew SF**, **Wong MY**, **Tam WL**, **Ip YK**. The snakehead *Channa asiatica* accumulates alanine during aerial exposure, but is incapable of sustaining locomotory activities on land through partial amino acid catabolism. *J Exp Biol* 206: 693–704, 2003.

11. **Clark AJ**, **Summers AP**. Morphology and kinematics of feeding in hagfish: possible functional advantages of jaws. *J Exp Biol* 210: 3897–3909, 2007.

12. **Clifford AM**, **Bury NR**, **Schultz AG**, **Ede JD**, **Goss BL**, **Goss GG**. Regulation of plasma glucose and sulfate excretion in Pacific hagfish, *Eptatretus stoutii* is not mediated by 11-deoxycortisol. *Gen. Comp. Endocrinol.* (January 23, 2017). doi: 10.1016/j.ygcen.2017.01.022.

13. **Clifford AM**, **Goss GG**, **Roa JN**, **Tresguerres M**. Acid/base and ionic regulation in hagfish. In: *Hagfish Biology*, edited by Edwards SL, Goss GG. Boca Raton, Fl: CRC Press, 2015, p. 277–298.

14. **Clifford AM**, **Goss GG**, **Wilkie MP**. Adaptations of a deep sea scavenger: High ammonia tolerance and active NH_4^+ excretion by the Pacific hagfish (*Eptatretus stoutii*). *Comp Biochem Physiol A* 182C: 64–74, 2015.

15. **Clifford AM**, **Guffey SC**, **Goss GG**. Extrabranchial mechanisms of systemic pH recovery in hagfish (*Eptatretus stoutii*). *Comp Biochem Physiol A* 168: 82–89, 2014.

16. **Clifford AM**, **Zimmer AM**, **Wood CM**, **Goss GG**. It's all in the gills: Evaluation of O2 uptake in Pacific hagfish refutes a major respiratory role for the skin. *J. Exp. Biol.* (July 8, 2016). doi: 10.1242/jeb.141598.

17. **Collins MA**, **Yau C**, **Nolan CP**, **Bagley PM**, **Priede IG**. Behavioural observations on the scavenging fauna of the Patagonian slope. *J Mar Biol Assoc UK* 79: 963–970, 1999.

18. **Cox GK**, **Sandblom E**, **Richards JG**, **Farrell AP**. Anoxic survival of the Pacific hagfish (*Eptatretus stoutii*). *J Comp Physiol B* 181: 361–371, 2011.

19. **Currie S**, **Edwards SL**. The curious case of the chemical composition of hagfish tissues-50 years on. *Comp Biochem Physiol A* 157: 111–115, 2010.

20. **Dvorak AM**, **Aird WC**. Endothelium in hagfish. In: *Hagfish Biology*, edited by Edwards SL, Goss GG. Boca Raton, FL: CRC Press, 2015, p. 161–206.

21. **Edgar RC**. MUSCLE: multiple sequence alignment with high accuracy and high throughput. *Nucl Acids Res* 32: 1792–1797, 2004.

22. **Edwards SL**, **Arnold J**, **Blair SD**, **Pray M**, **Bradley R**, **Erikson O**, **Walsh PJ**. Ammonia excretion in the Atlantic hagfish (*Myxine glutinosa*) and responses of an Rhc glycoprotein. *Am J Physiol Regul Integr Comp Physiol* 308: R769–78, 2015.

23. **Evans DH**. Gill Na^+/H^+ and Cl^-/HCO_3^- exchange systems evolved before the vertebrates entered fresh water. *J Exp Biol* 113: 465–469, 1984.

24. **Frick NT**, **Wright PA**. Nitrogen metabolism and excretion in the mangrove killifish *Rivulus marmoratus* II. Significant ammonia volatilization in a teleost during air-exposure. *J Exp Biol* 205: 91–100, 2002.

25. **Galtier N**, **Gouy M**, **Gautier C**. SEAVIEW and PHYLO_WIN: two graphic tools for sequence alignment and molecular phylogeny. *Comput Appl Biosci* 12: 543–548, 1996.

26. **Glover C**, **Bucking C**, **Wood C**. Adaptations to *in situ* feeding: novel nutrient

acquisition pathways in an ancient vertebrate. *Proc R Soc B* 278: 3096–3101, 2011.

27. **Gouy M**, **Guindon S**, **Gascuel O**. SeaView version 4: A multiplatform graphical user interface for sequence alignment and phylogenetic tree building. *Mol Biol Evol* 27: 221–224, 2010.

28. **Hans M**, **Tabencka Z**. Über die Blutgefässe der Haut *Myxine glutinosa* L. *Bull Acad Pol Sci* Ser. BII Zool: 69–77, 1938.

29. **Ip Y**, **Chew S**, **Leong I**, **Jin Y**, **Lim C**, **Wu R**. The sleeper *Bostrichthys sinensis* (Family Eleotridae) stores glutamine and reduces ammonia production during aerial exposure. *J Comp Physiol B* 171: 357–367, 2001.

30. **Ip YK**, **Randall DJ**, **Kok TKT**, **Barzaghi C**, **Wright PA**, **Ballantyne JS**, **Wilson JM**, **Chew SF**. The giant mudskipper *Periophthalmodon schlosseri* facilitates active NH_4^+ excretion by increasing acid excretion and decreasing NH_3 permeability in the skin. *J Exp Biol* 207: 787–801, 2004.

31. **Laemmli UK**. Cleavage of structural proteins during the assembly of the head of bacteriophage T4. *Nature* 227: 680–685, 1970.

32. **Lametschwandtner A**, **Weiger T**, **Lametschwandtner U**, **Georgieva-Hanson V**, **Patzner RA**, **Adam H**. The vascularization of the skin of the Atlantic hagfish, *Myxine glutinosa* L. as revealed by scanning electron microscopy of the vascular corrosion casts. *Scanning Microsc* 3: 305–314, 1989.

33. **Le SQ**, **Gascuel O**. An improved general amino acid replacement matrix. *Mol Biol Evol* 25: 1307–1320, 2008.

34. **Malte H**, **Lomholt JP**. Ventilation and gas exchange. In: *The Biology of Hagfishes*, edited by Jørgensen JM, Lomholt JP, Weber RE, Malte H. Dordrecht: Springer Netherlands, 1998, p. 223–234.

35. **Martini FH**. The ecology of hagfishes. In: *The Biology of Hagfishes*. Dordrecht: Springer Netherlands, 1998, p. 57–77.

36. **McDonald DG**, **Cavdek V**, **Calvert L**, **Milligan CL**. Acid-base regulation in the Atlantic hagfish *Myxine glutinosa*. *J Exp Biol* 161: 201–215, 1991.

37. **Miller MA**, **Pfeiffer W**, **Schwartz T**. Creating the CIPRES Science Gateway for inference of large phylogenetic trees. *Proceedings of the Gateway Computing Environments Workshop* (November 14, 2010). doi: 10.1109/GCE.2010.5676129.

38. **Morris R**. Studies on salt and water balance in *Myxine glutinosa* (L.). *J Exp Biol* 42: 359–371, 1965.

39. **Potter IC**, **Welsch U**, **Wright GM**, **Honma Y**, **Chiba A**. Light and electron

microscope studies of the dermal capillaries in three species of hagfishes and three species of lampreys. *J Zool* 235: 677–688, 1995.

40. **Rauther M**. Kiemen der anamnier-kiemendarm-derivate der Cyclostomen und fische. die driisenartigen derivate des kiemendarmes und kiemengange bei den Cyclostomen und fischen. In: *Handbuch der vergleichenden Anatomie der Wirbeltiere*. Berlin: Urban & Schwarzenberg, 1937, p. 211–278.

41. **Sayer MDJ**, **Davenport J**. The relative importance of the gills to ammonia and urea excretion in five seawater and one freshwater teleost species. *J Fish Biol* 31: 561–570, 1987.

42. **Schultz AG**, **Guffey SC**, **Clifford AM**, **Goss GG**. Phosphate absorption across multiple epithelia in the Pacific hagfish (*Eptatretus stoutii*). *Am J Physiol Regul Integr Comp Physiol* 307: R643–652, 2014.

43. **Smart G**. The effect of ammonia exposure on gill structure of the rainbow trout (*Salmo gairdneri*). *J. Fish Biol.* (1976). doi: 10.1111/j.1095-8649.1976.tb03990.x/pdf.

44. **Smith CR**, **Baco AR**. Ecology of whale falls at the deep-sea floor. *Oceanogr Mar Biol* 41: 311–354, 2003.

45. **Stamatakis A**. RAxML version 8: a tool for phylogenetic analysis and post-analysis of large phylogenies. *Bioinformatics* 30: 1312–1313, 2014.

46. **Strahan R**. The Behaviour of Myxinoids. *Acta Zoologica* 44: 73–102, 1963.

47. **Talavera G**, **Castresana J**. Improvement of phylogenies after removing divergent and ambiguously aligned blocks from protein sequence alignments. *Syst Biol* 56: 564–577, 2007.

48. **Tsui T**, **Randall DJ**, **Chew SF**, **Jin Y**, **Wilson JM**, **Ip YK**. Accumulation of ammonia in the body and NH_3 volatilization from alkaline regions of the body surface during ammonia loading and exposure to air in the weather loach *Misgurnes anguillicaudatus*. *J Exp Biol* 651-659, 2002.

49. **Verdouw H**, **Van Echteld C**, **Dekkers E**. Ammonia determination based on indophenol formation with sodium salicylate. *Water Res* 12: 399–402, 1978.

50. **Walsh PJ**, **Veauvy CM**, **McDonald MD**, **Pamenter ME**, **Buck LT**, **Wilkie MP**. Piscine insights into comparisons of anoxia tolerance, ammonia toxicity, stroke and hepatic encephalopathy. *Comp Biochem Physiol A* 147: 332–343, 2007.

51. **Weiner ID**, **Verlander JW**. Ammonia transport in the kidney by Rhesus glycoproteins. *Am J Physiol Renal Physiol* 306: F1107–20, 2014.

52. **Weinrauch AM**, **Edwards SL**, **Goss GG**. Anatomy of the Pacific hagfish

(*Eptatretus stoutii*). In: *Hagfish Biology*, edited by Edwards SL, Goss GG. Boca Raton: CRC Press, 2015, p. 1–40.

53. **Welsch U**, **Potter IC**. Dermal capillaries. In: *The Biology of Hagfishes*. Dordrecht: Springer Netherlands, 1998, p. 273–283.

54. **Wilkie MP**, **Stecyk JAW**, **Couturier CS**, **Sidhu S**, **Sandvik GK**, **Nilsson GE**. Reversible brain swelling in crucian carp (*Carassius carassius*) and goldfish (*Carassius auratus*) in response to high external ammonia and anoxia. *Comp Biochem Physiol A* 184: 65–75, 2015.

55. **Wilson RW**, **Taylor EW**. Transbranchial ammonia gradients and acid-base responses to high external ammonia concentration in rainbow trout (*Oncorhynchus mykiss*) acclimated to different salinities. *J Exp Biol* 166: 95–112, 1992.

56. **Wright PA**, **Wood CM**. A new paradigm for ammonia excretion in aquatic animals: role of Rhesus (Rh) glycoproteins. *J Exp Biol* 212: 2303–2312, 2009.

57. **Zimmer AM**, **Brauner CJ**, **Wood CM**. Ammonia transport across the skin of adult rainbow trout (*Oncorhynchus mykiss*) exposed to high environmental ammonia (HEA). *J Comp Physiol B* 184: 77–90, 2014.

Figure Captions

Figure 1. Changes in (A) plasma [T_{Amm}] and (B) blood pH of Pacific hagfish exposed to HEA (closed bars; 20 mmol L^{-1}) for 48 h and following a 4 h recovery in ammonia-free, full strength seawater within divided chambers. Control fish (No-HEA; open bars) were housed in ammonia-free seawater for the exposure period. Blood was drawn immediately prior to HEA exposure (Pre-exposure), following HEA exposure (0 h) and following a 4 h recovery period (4 h). Following blood sampling at 0 h, a sub-set of HEA exposed hagfish were fitted with a cloacal seal (HEA seal; light gray bars), while the other group was left untreated (HEA no seal; dark gray bars) prior to being positioned into divided flux chambers. Data are presented as mean + s.e.m. (n = 8 unless otherwise specified. Bars with same letter are not statistically different ($p < 0.05$) as determined by two-way ANOVA followed by Holm-Sidak's multiple comparisons *post hoc* test with all possible comparisons made.

Figure 2. Partitioning of net outward ammonia excretion (J_{Amm}) in Pacific hagfish exposed to HEA (20 mmol L^{-1}) for 48 h during recovery in ammonia-free, full strength seawater within divided chambers. Control fish (No-HEA; open bars) were housed in ammonia-free seawater for the duration of the exposure period. J_{Amm} was measured in the (A) anterior and (B) posterior chambers during the 4 h recovery period. Data are presented as mean + s.e.m. (n). Bars with same letter are not statistically different ($p < 0.05$) as determined by one-way ANOVA followed by Holm-Sidak's multiple comparisons *post hoc* test. Details of cloacal seal application are described in Figure 1.

Figure 3. Changes in (A) plasma [T_{Amm}] and (B) blood pH following during localized exposure of hagfish to HEA (20 mM) via either ammonia-free seawater (no HEA; open bars) or 20 mmol L^{-1} T_{Amm} in either the anterior compartment (HEA in front) or the posterior compartment (HEA in back) divided chamber. Blood samples were drawn immediately following the 48 h exposure. Data are presented as mean + s.e.m. (*n*). Bars with same letter are not statistically different ($p < 0.05$) as determined by a Kruskal-Wallis non-parametric test followed my Dunn's multiple comparison test in (A) and by one-way ANOVA followed by Holm-Sidak's multiple comparisons *post hoc* test in (B).

Figure 4. Ammonia excretion during localized HEA exposure. Net outward (A) anterior and (B) posterior J_{Amm} from hagfish during acute localized HEA exposure was determined in the compartment opposite to the HEA-containing compartment. Data are presented as mean + s.e.m. (*n*). Bars with same letter are not statistically different ($p < 0.05$) as determined by Student's one-tailed t-test.

Figure 5. Total ammonia flux across excised skin as determined by appearance of ammonia in mucosal medium following introduction to serosal HEA (0.05 – 10.0 mmol L^{-1} in hagfish saline). Concentration-dependent flux (A) was determined in excised skin from hagfish ($n = 6$) either pre-exposed to HEA (20 mmol L^{-1}) for 48 h (closed bars) or non-exposed controls (open bars). Skin J_{Amm} was measured in skin excised from serial sections along the length of non-HEA exposed animals. The serosal side of skin sections were then exposed to 5 mmol L^{-1} T_{Amm}in hagfish saline, and the appearance of ammonia

839 measured on the mucosal side of the chamber. Data are presented as mean + s.e.m. in (A)
840 and mean ± s.e.m. in (B). Statistical differences in (A) are denoted by asterisks (*; $p <$
841 0.05) as determined by multiple Student's t-tests with a Holm-Sidak multiple
842 comparisons correction. Solid line in (B) represents line of best fit as determined by
843 linear regression analysis (equation: Skin J_{Amm} = 0.1307 ([nmol cm^{-1} h^{-1}]/[% distance
844 from snout]) + 18.82 nmol cm^{-1} h^{-1}); broken lines represent 95% confidence limits for
845 line of best fit and the shaded area represents the placement of collar assembly on hagfish
846 in separating chamber protocols.
847
848 Figure 6. Phylogenetic analysis of 2 cloned Rh glycoprotein sequences showed
849 phylogenetic relationships of *Es*Rhcg and *Es*Rh-like peptide sequences. Analysis was
850 completed using RAx-ML with methods previously described on the Cyberinfrastructure
851 for Phylogenetic Research (CIPRES) Science Gateway servers. Branch support was
852 estimated by bootstrap with 300 replications with auto-cutoff threshold set to 1000.
853 Cloned sequences are denoted with an arrow. Numbers in square brackets are the
854 GenBank accession numbers of the sequences.
855
856 Figure 7. Representative micrographs depicting Pacific hagfish cutaneous cellular
857 organization and *Es*Rhcg localization. Haematoxylin and eosin staining (A) highlighting
858 the large mucous cells (MC) and clearly defined basement membrane separating the
859 epidermis (Ep) from the capillary-rich (Cp; denoted by arrows) dermis (De).
860 Immunohistochemistry representative confocal images showing localization of the
861 *Es*Rhcg using *Myxinid*-derived antibodies (red) to the basal aspect of the epidermis (B).

Immunoreactivity was observed along the length of the basement membrane of the epidermis, extending up to surround the large mucous cells (MC). Pre-absorbed antibody control micrograph (B - inset) demonstrating no evidence of *Es*Rhcg staining. Scale bars = 100 μm in (A) and 20 μm in B.

Figure 8. Cutaneous distribution of *Es*Rhcg abundance in hagfish. Hagfish skin was excised in sequential sections (Anterior, Middle, Posterior) from along the length of the animal. Skin sections were distributed by percentage distance from the snout (Anterior: 27.58 ± 0.9 %; Middle: 57.21 ± 1.40 %; Posterior: 84.19 ± 1.08 %). (A) Representative blot from anterior, middle and posterior skin sections. (B) Relative abundance of cutaneous *Es*Rhcg expression from sequential skin sections. Data are presented as mean + s.e.m (n). Bars with same letter are not statistically different ($p < 0.05$) as determined by one-way ANOVA followed by Holm-Sidak's multiple comparisons *post-hoc* test.

Tables

Table 1 List of Rh sequences used for HMMER search

Rh glycoprotein sequences used to construct HMM profiles for HMMER search querying hagfish illumina transcriptomes. Sequences were acquired from NCBI GenBank repository

Isoform	Species	Accession #
Rhbg	*Takifugu rubripes*	AAM48577.1
	Alcolapia grahami	AFZ78445.1
	Cyprinus carpio	AGM46574.1
	Porichthys notatus	AGA93879.1
	Opsanus beta	AEA77168.1
	Bos taurus	AAI33319.1
	Rattus norvegicus	AAH79365.1
	Oryzias latipes	NP_001098561.1
	Danio rerio	NP_956365.2
	Takifugu rubripes	AAM48577.1
	Porichthys notatus	AGA93879.1
	Ophiophagus hannah	ETE58616.1
	Xenopus tropicalis	AAU89493.1
	Pan troglodytes	AAX39716.1
	Tetraodon nigroviridis	Q3BBX8.1
Rhcg	*Takifugu rubripes*	Q18PF5.1
	Danio rerio	NP_001083046.1
	Oncorhynchus mykiss	NP_001117995.1
	Oreochromis niloticus	XP_003442301.1
	Opsanus beta	AEA77169.1
	Gallus gallus	NP_001004370.1
	Monodelphis domestica	XP_001369976.1
	Xenopus tropicalis	NP_001003661.1
	Sus scrofa	NP_001038042.1
	Anolis carolinensis	XP_003227100.1
	Canis lupus familiaris	NP_001041487.1
	Pan troglodytes	NP_001030600.1
	Homo sapiens	NP_057405.1

880 **Table 2 List of primers used for PCR amplification.**

Application		Sequences
*Es*Rhcg		
PCR set	sense:	5’- CCTGCTGTATAACCGGTCGATATT -3’
Full CDS	antisense:	5’- CCAATGGAGCTTGCACCAAATAG -3’
*Es*Rh-like		
PCR set	sense:	5’-CAACTCCGAGCTTCGCAA-3’
Full CDS	antisense:	5’-TGCCTGTATGTCTGCTTGTATG-3’

881

882 **Table 3 Comparison of hagfish Rhcg antibody binding domain**

Species	Peptide sequence
Myxine glutinosa	5'-CYEDRAYWEVPEEEVTY-3'
Eptatretus stoutii	5'-CYEDEAYWEVPEEEVTL-3'

883

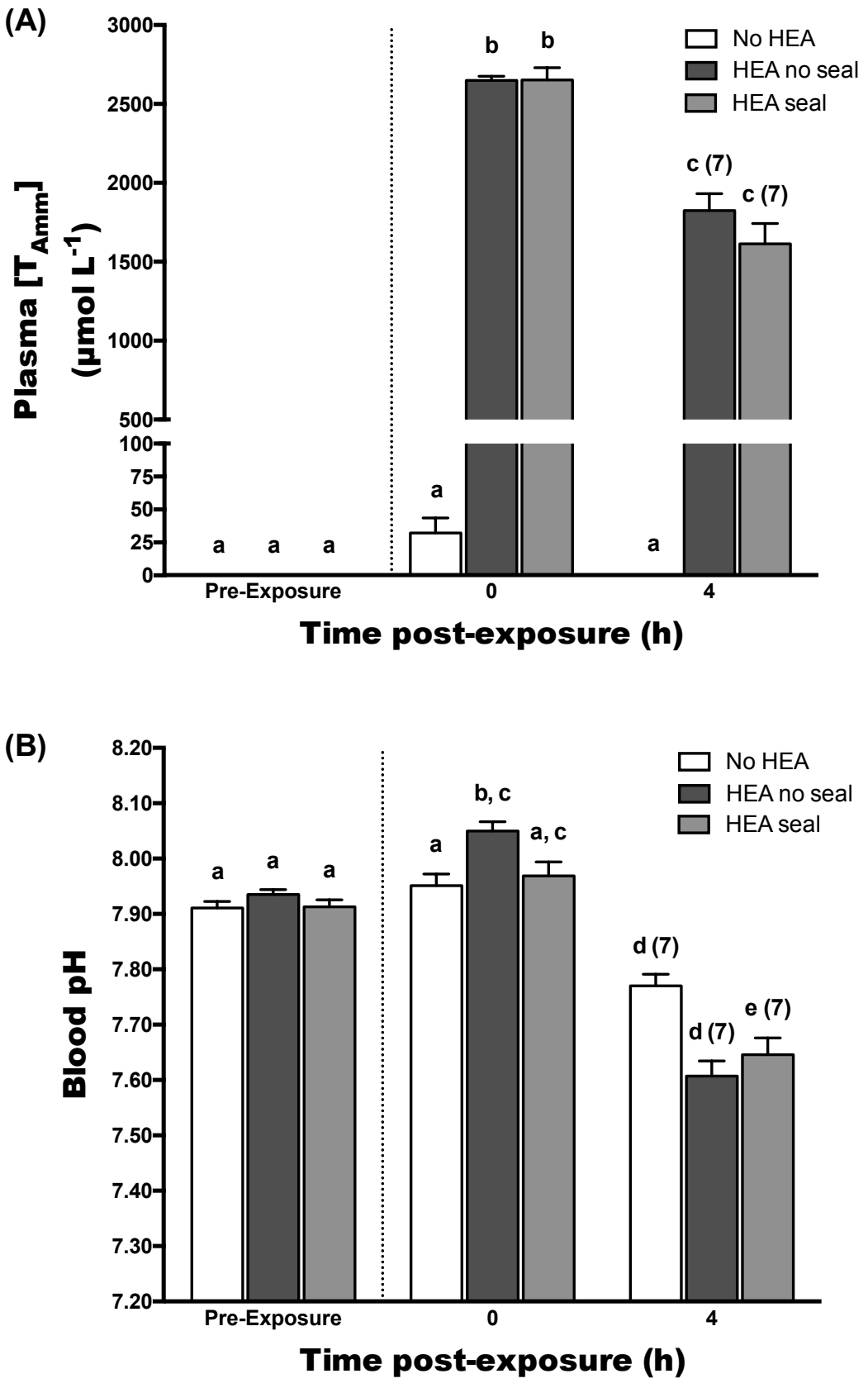
(A)
Plasma [T_{Amm}] (μmol L^{-1})
3000
2500
2000
1500
1000
500
100
75
50
25
0
No HEA
HEA no seal
HEA seal
b
b
c (7)
c (7)
a
a
a
a
Pre-Exposure
0
4
Time post-exposure (h)
(B)
Blood pH
8.20
8.10
8.00
7.90
7.80
7.70
7.60
7.50
7.40
7.30
7.20
No HEA
HEA no seal
HEA seal
a
a
a
a
b, c
a, c
d (7)
d (7)
e (7)
Pre-Exposure
0
4
Time post-exposure (h)

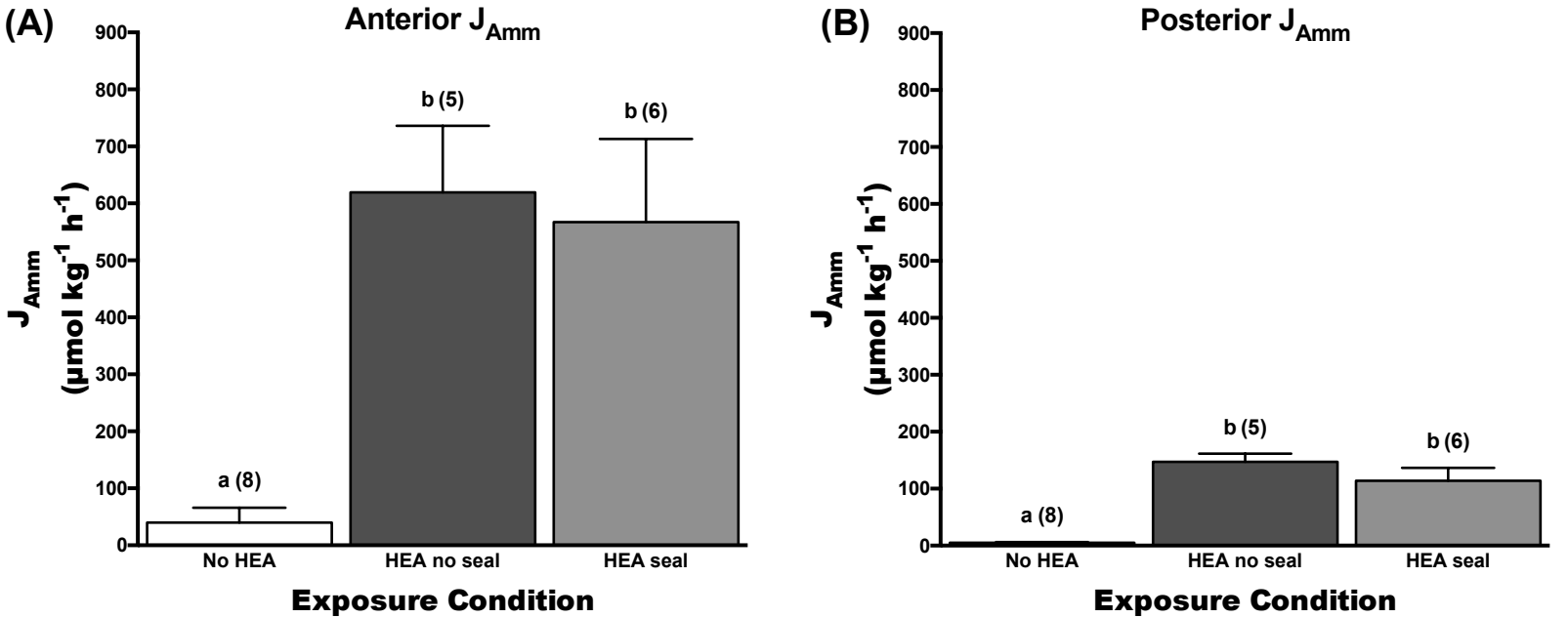
(A)
Anterior J_{Amm}
J_{Amm} (µmol kg^{-1} h^{-1})
900
800
700
600
500
400
300
200
100
0
a (8)
b (5)
b (6)
No HEA
HEA no seal
HEA seal
Exposure Condition
(B)
Posterior J_{Amm}
J_{Amm} (µmol kg^{-1} h^{-1})
900
800
700
600
500
400
300
200
100
0
a (8)
b (5)
b (6)
No HEA
HEA no seal
HEA seal
Exposure Condition

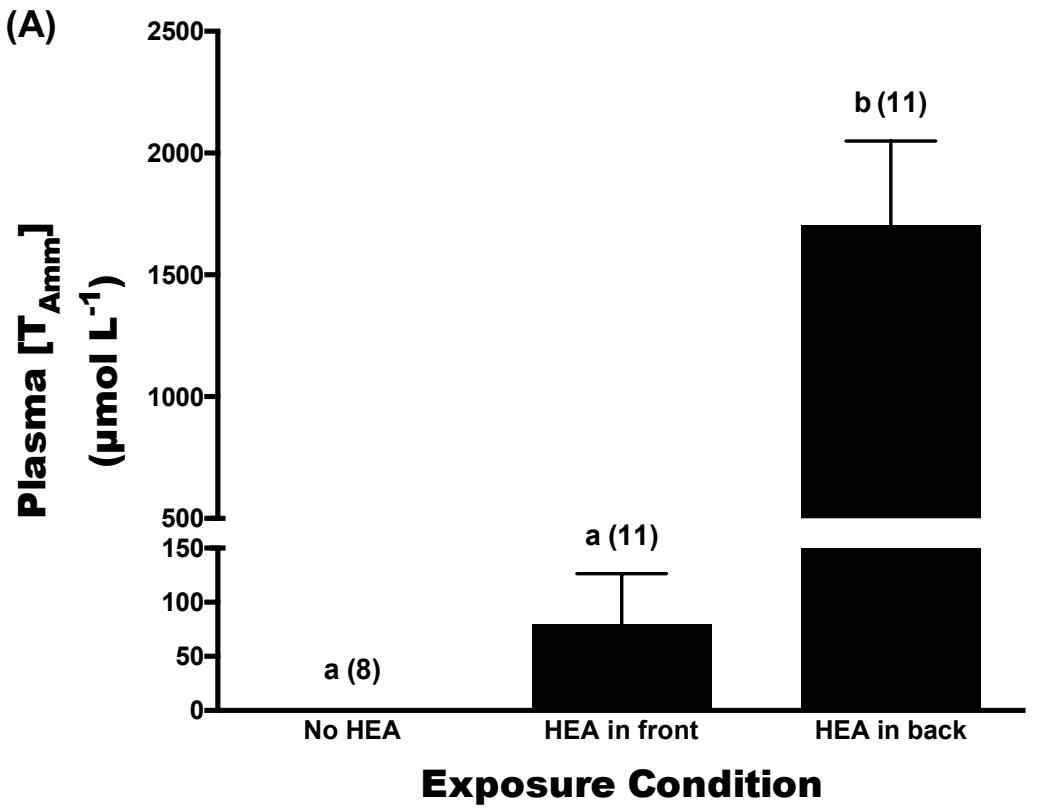
(A)
2500
2000
1500
1000
500
150
100
50
0
Plasma [T_{Amm}] (µmol L^{-1})
b (11)
a (11)
a (8)
No HEA
HEA in front
HEA in back
Exposure Condition

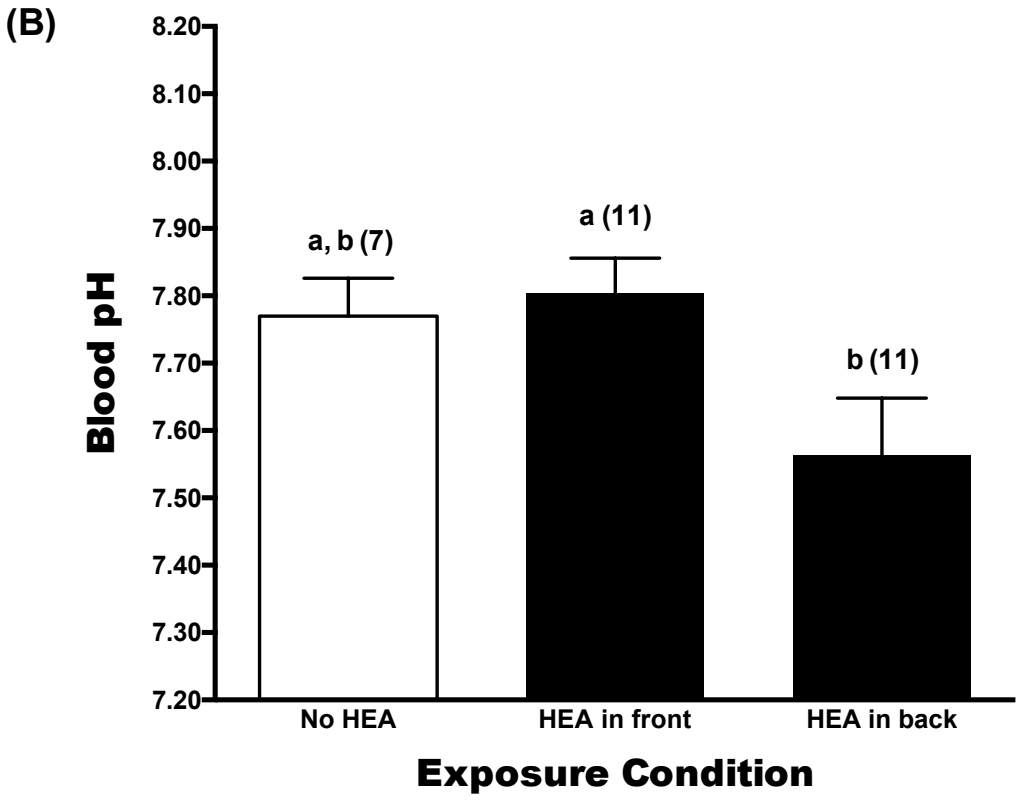
(B)
8.20
8.10
8.00
7.90
7.80
7.70
7.60
7.50
7.40
7.30
7.20
Blood pH
a, b (7)
a (11)
b (11)
No HEA
HEA in front
HEA in back
Exposure Condition

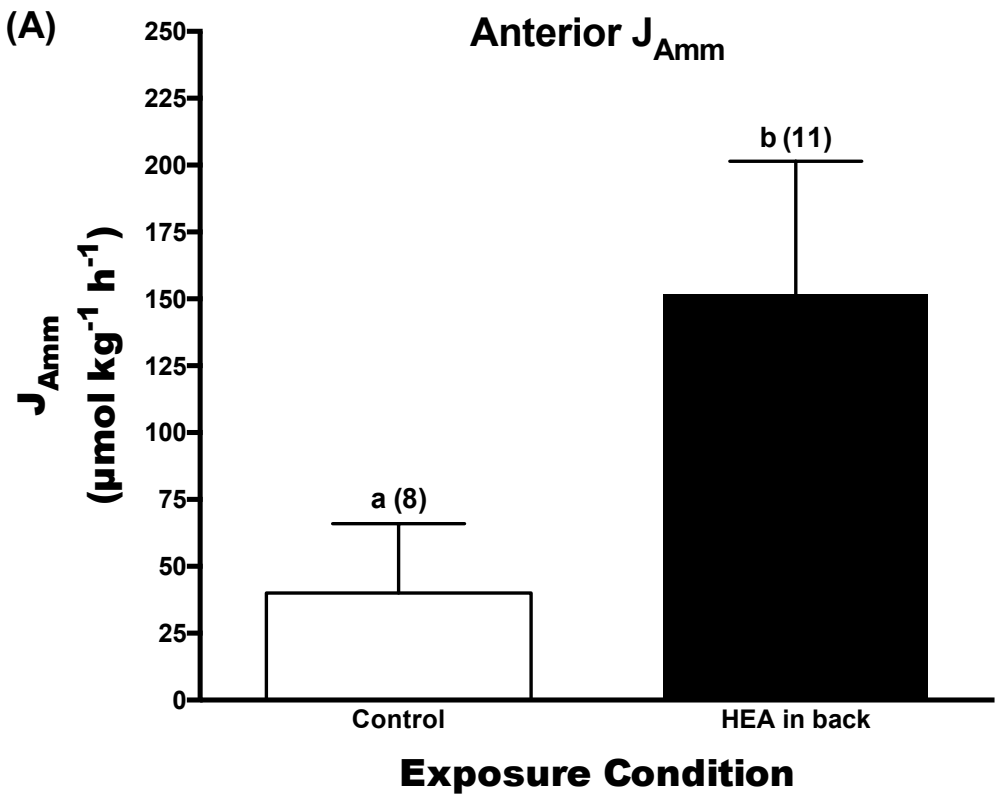
(A)
Anterior J_{Amm}
250
225
200
175
150
125
100
75
50
25
0
J_{Amm} (µmol kg^{-1} h^{-1})
a (8)
b (11)
Control
HEA in back
Exposure Condition

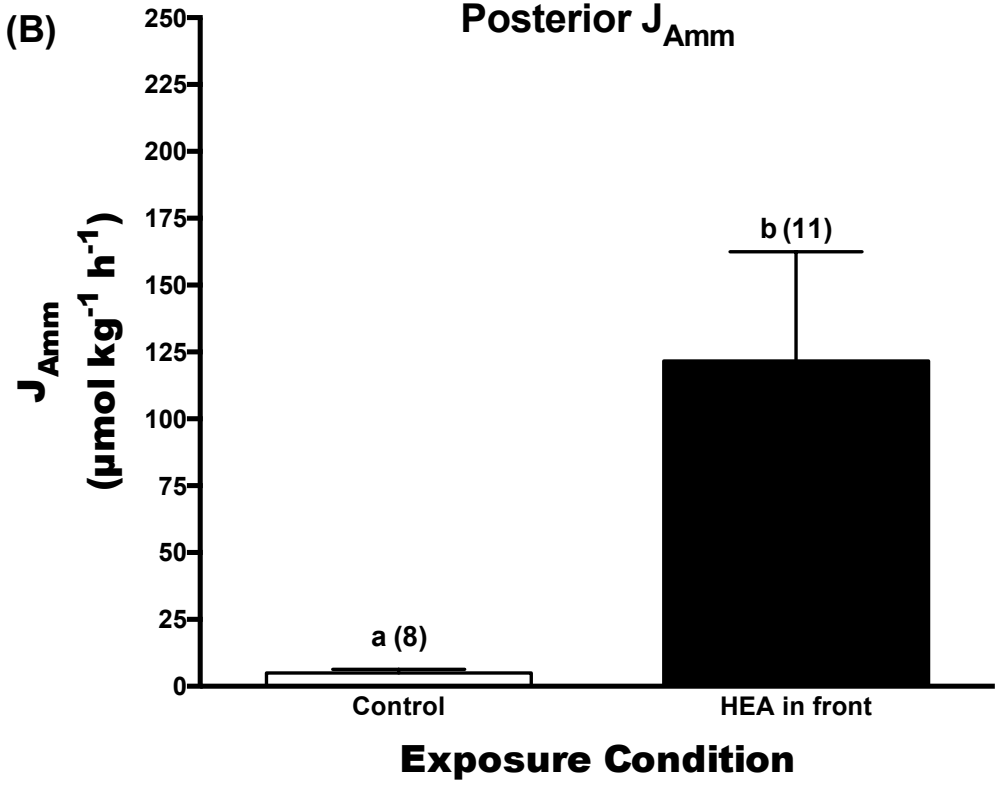
(B)
Posterior J_{Amm}
250
225
200
175
150
125
100
75
50
25
0
J_{Amm} (µmol kg^{-1} h^{-1})
a (8)
b (11)
Control
HEA in front
Exposure Condition

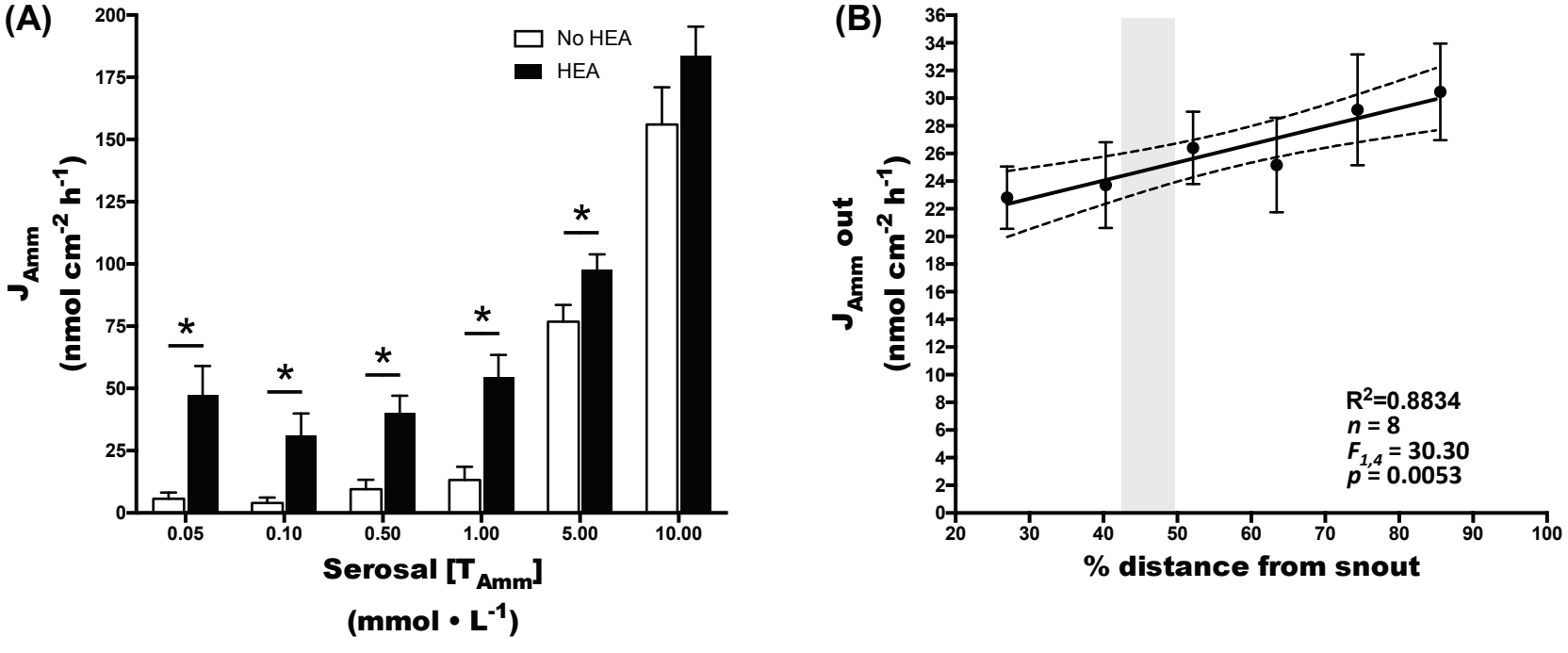
(A)
No HEA
HEA
J_{Amm} (nmol cm^{-2} h^{-1})
200
175
150
125
100
75
50
25
0
*
0.05
0.10
0.50
1.00
5.00
10.00
Serosal [T_{Amm}] (mmol • L^{-1})
(B)
J_{Amm} out (nmol cm^{-2} h^{-1})
36
34
32
30
28
26
24
22
20
18
16
14
12
10
8
6
4
2
0
R^2=0.8834
n = 8
$F_{1,4}$ = 30.30
p = 0.0053
20
30
40
50
60
70
80
90
100
% distance from snout


Rh-like Nitrosomonas europaea [WP_011111083.1]
Rh50A Drosophila melanogaster [NP_647940.1]
Rh-like Drosophila melanogaster [AAF19374.1]
Rh-like1 Caenorhabditis elegans [AAF97864.1]
Rh-like2 Caenorhabditis elegans [AAF97865.1]
Rhag Ciona intestinalis [AAP42763.1]
Rhbg-like Ciona savignyi [AAY41909.1]
Rhcg Ciona intestinalis [AAP42761.1]
Rhbg Ciona intestinalis [AAP42762.1]
Rhcg-like Ciona savignyi [AAY41908.1]
Rhp2 Triakis scyllium [BAI49727.1]
Rh-like Tetraodon nigroviridis [AAY81950.1]
Rhag1 Takifugu rubripes [AAM48575.1]
Rh50-like Danio rerio [AAF63256.1]
Rhag2 Takifugu rubripes [AAM48576.1]
Rh30-like2 Takifugu rubripes [AAU81656.1]
Rhp Xenopus tropicalis [AAY41904.1]
Rh-like Eptatretus stoutii [KT943754]
Rhbg Myxine glutinosa [ADD63336.1]
Rh30-like Danio rerio [AAU81655.1]
Rhag-like Salmo salar [AAR01778.1]
Rh30-like3 Oncorhynchus mykiss [ABN73108.1]
Rh30-like2 Oncorhynchus mykiss [ABN73107.1]
Rh30 Tetraodon nigroviridis [AAY41905.1]
Rh30-like1 Takifugu rubripes [AAM48580.2]
Rhag-precursor Mus musculus [NP_035399.1]
Rhag Rattus norvegicus [NP_075411.2]
Rhag Canis familiaris [NP_001104238.1]
Rhag Macaca mulatta [NP_001027987.1]
Rh50 Pongo pygmaeus [AAG00305.1]
Rh50 Gorilla gorilla [AAG00304.1]
Rh50 Homo sapiens [AAF78209.1]
Rhag Pan troglodytes [NP_001009033.1]
Rhag Danio rerio [NP_998010.1]
Rhag-like Takifugu rubripes [AAV28817.1]
Rhag Gasterosteus aculeatus [ABF69688.1]
Rhag Oncorhynchus mykiss [ABV24962.1]
Rhcg Myxine glutinosa [ADD63335.1]
Rhcg Eptatretus stoutii [KT943755]
Rhcg Sus scrofa [ABF69687.1]
Rhcg Canis familiaris [NP_001041487.1]
RhCG Homo sapiens [AAH30965.1]
Rhcg Pan troglodytes [AAX39717.1]
Rhcg Macaca mulatta [ABD72472.1]
Rhcg Oryctolagus cuniculus [AAK14652.1]
Rhcg Rattus norvegicus [AAN07791.1]
Rhcg Mus musculus [NP_062773.2]
Rhcg Xenopus tropicalis [AAQ02688.1]
Rhcg2a Danio rerio [BAF63791.1]
Rhcg2c Danio rerio [BAF63792.1]
Rhcg Oncorhynchus mykiss [AAU89494.1]
Rhcg2 Takifugu rubripes [AAM48579.1]
Rhcg Oryzias latipes [BAB13346.1]
Rhcg2 Kryptolebias marmoratus [ABD83662.1]
Rhcg Gasterosteus aculeatus [ABF69690.1]
Rhcg1a Oncorhynchus mykiss [ABD92924.1]
Rhcg1 Danio rerio [BAF63790.1]
Rhcg1b Danio rerio [AAM90586.1]
Rhcg1 Takifugu rubripes [AAM48578.1]
Rhcg Tetraodon nigroviridis [AAY41907.1]
Rhcg1 Kryptolebias marmoratus [ABN41463.1]
Rhbg-b Oncorhynchus mykiss [ABO16486.1]
Rhbg-a Oncorhynchus mykiss [ABO16485.1]
Rhbg Kryptolebias marmoratus [ABO18606.1]
Rhbg Oryzias latipes [AAR08676.1]
Rhp2 Gasterosteus aculeatus [ABF69691.1]
Rhbg Gasterosteus aculeatus [ABF69689.1]
Rhbg Tetraodon nigroviridis [AAY41906.1]
Rhbg Takifugu rubripes [AAM48577.1]
Rhbg Takifugu rubripes [BAE96342.1]
Rhbg Danio rerio [AAQ09527.1]
Rhbg Xenopus tropicalis [AAU89493.1]
Rhbg Canis familiaris [AAN76725.1]
Rhbg-precursor Canis familiaris [NP_001003017.2]
Rhbg-precursor Sus scrofa [NP_999161.1]
Rhbg Oryctolagus cuniculus [AAK14652.1]
Rhbg Rattus norvegicus [AAH79365.1]
Rhbg-precursor Mus musculus [NP_067350.2]
Rhbg Macaca mulatta [AAL56017.1]
Rhbg Gorilla gorilla [AAK16202.1]
Rhbg Pongo pygmaeus [AAK16204.1]
Rhbg Hylobates sp. [AAK16203.1]
RhBG2a Homo sapiens [AAN34364.1]
RhBGa Homo sapiens [NP_065140.3]
Rhbg Pan troglodytes [AAX39716.1]
0.2

(A)

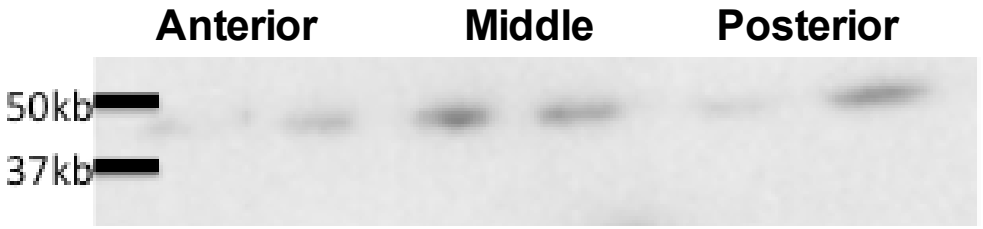
Anterior
Middle
Posterior
50kb
37kb

(B)

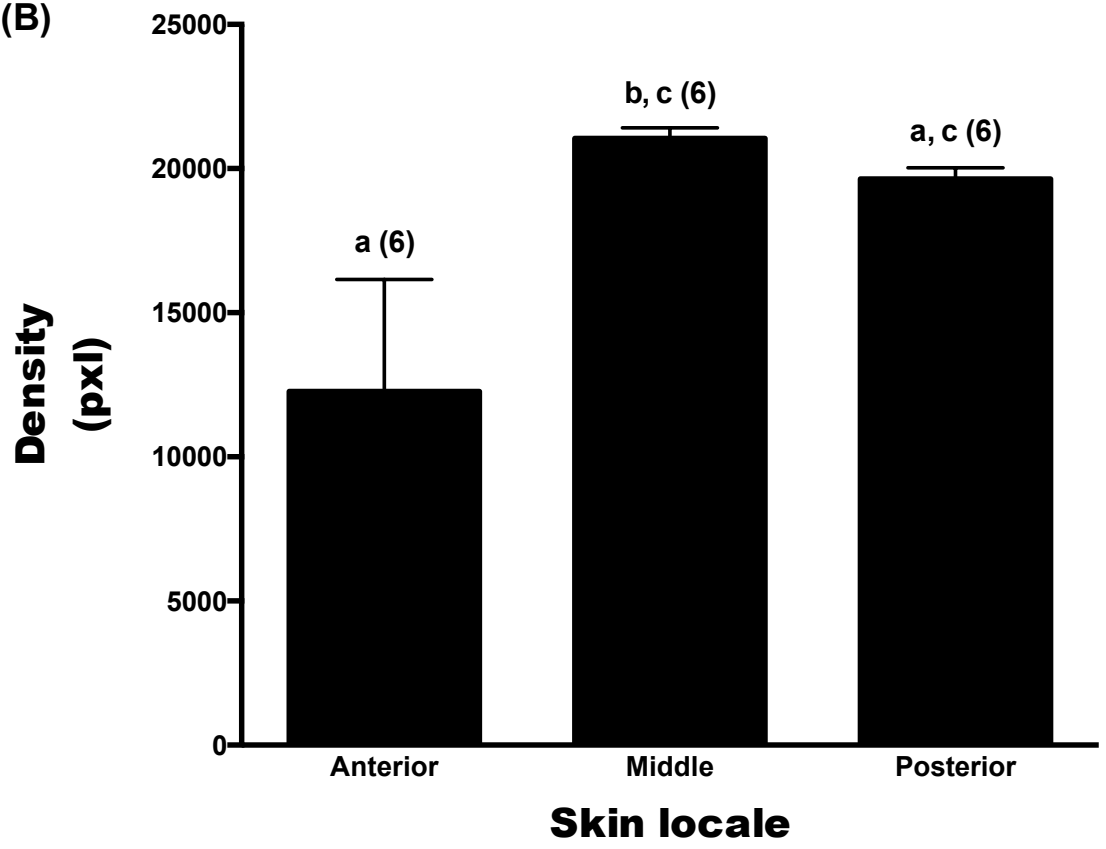
25000
20000
15000
10000
5000
0
Density (pxl)
a (6)
b, c (6)
a, c (6)
Anterior
Middle
Posterior
Skin locale